Homeostatic MyD88-dependent signals cause lethal inflammation in the absence of A20

Emre E. Turer,[1] Rita M. Tavares,[1,2] Erwan Mortier,[1] Osamu Hitotsumatsu,[1] Rommel Advincula,[1] Bettina Lee,[1] Nataliya Shifrin,[1] Barbara A. Malynn,[1] and Averil Ma[1]

[1]Gastrointestinal Division, Department of Medicine, Biomedical Sciences Program, University of California, San Francisco, San Francisco, CA 94143
[2]Ph.D. Programme in Biomedicine, Instituto Gulbenkian de Ciência, 2781-901 Oeiras, Portugal

Toll-like receptors (TLRs) on host cells are chronically engaged by microbial ligands during homeostatic conditions. These signals do not cause inflammatory immune responses in unperturbed mice, even though they drive innate and adaptive immune responses when combating microbial infections. A20 is a ubiquitin-modifying enzyme that restricts exogenous TLR-induced signals. We show that MyD88-dependent TLR signals drive the spontaneous T cell and myeloid cell activation, cachexia, and premature lethality seen in A20-deficient mice. We have used broad spectrum antibiotics to demonstrate that these constitutive TLR signals are driven by commensal intestinal flora. A20 restricts TLR signals by restricting ubiquitylation of the E3 ligase tumor necrosis factor receptor–associated factor 6. These results reveal both the severe proinflammatory pathophysiology that can arise from homeostatic TLR signals as well as the critical role of A20 in restricting these signals in vivo. In addition, A20 restricts MyD88-independent TLR signals by inhibiting Toll/interleukin 1 receptor domain–containing adaptor inducing interferon (IFN) β–dependent nuclear factor κB signals but not IFN response factor 3 signaling. These findings provide novel insights into how physiological TLR signals are regulated.

CORRESPONDENCE
Averil Ma:
averil.ma@ucsf.edu

Abbreviations used: BMDM, bone marrow–derived macrophage; HSC, hematopoietic stem cell; IRAK-M, IL-1R–associated kinase M; IRF, IFN response factor; MCP, monocyte chemoattractant protein; mRNA, messenger RNA; PAMP, pathogen-associated molecular pattern; poly (I:C), poly-inosine:cytosine; RIP, receptor-interacting protein; R.U., relative units; SIGIRR, single Ig and TIR domain; SOCS, suppressor of cytokine signaling; TIR, Toll/IL-1 receptor; TLR, Toll-like receptor; TRAF, TNF receptor–associated factor; TRIF, TIR domain–containing adaptor inducing IFN-β.

Higher eukaryotes are colonized by microbial organisms, predominantly on interfaces with the environment such as the skin and gastrointestinal tract (1). Recent studies suggest that host cells, including professional antigen-presenting cells, "sense" the presence of microbial molecules under homeostatic conditions (2, 3). This sensing is performed by several families of cellular receptors, including Toll-like receptors (TLRs) and non-TLR proteins such as NOD/CATERPILLAR family proteins (4, 5). Collectively, these proteins are thought to bind to conserved pathogen-associated molecular patterns (PAMPs) and activate proinflammatory signals in host cells. The appreciation that microbial sensors such as TLRs may chronically or tonically engage PAMPs during homeostasis raises a major question: if TLRs trigger both adaptive and innate immune responses, why do homeostatic TLR signals not trigger inflammation? Despite the presence of up to 10^{11} bacteria per gram of luminal contents within the gastrointestinal tract, most humans tolerate this colonization without adverse effects. Indeed, host cell sensing of luminal microbes may provide beneficial signals under homeostatic conditions (2). How immune responses to commensal flora are restrained during homeostasis thus remains one of the central questions in immune regulation.

Inflammatory TLR signals might be distinguished from homeostatic TLR signals by the quantity or strength of TLR signals, by cell type–specific responses, by the cellular location of PAMP/TLR interactions (e.g., apical vs. basal surfaces or intracellular vs. membrane-bound receptors), or by additional extracellular cues (e.g., cellular stress response proteins) that modify the cellular interpretation of such signals. Among these general mechanisms, perhaps the most attention has been focused on proteins that regulate the intracellular strength, duration, and/or character of PAMP-triggered signaling.

TLR proteins contain leucine-rich repeat regions that mediate ligand binding. TLRs also

E.E. Turer and R.M. Tavares contributed equally to this work.

contain intracellular Toll/IL-1 receptor (TIR) domains that trigger signals via homotypic interactions with proximal adaptor proteins (6, 7). All TLRs signal via the adaptor MyD88, leading to activation of NF-κB and mitogen-activated protein (MAP) kinase pathways. NF-κB activation leads to a transcriptional program that up-regulates proinflammatory gene products such as IL-1β and TNF-α and, ultimately, to the activation and accumulation of monocytes. MyD88 is essential for most TLR-induced NF-κB signaling, as MyD88-deficient ($MyD88^{-/-}$) cells exhibit reduced and delayed NF-κB signaling activity (8, 9). TLR3 and TLR4 also use another adaptor, TIR domain–containing adaptor inducing IFN-β (TRIF). TRIF-dependent signals activate IFN response factor 3 (IRF3) in addition to NF-κB (10, 11). These transcription factors induce productive antiviral immune responses by binding to promoters of type I IFN and chemotactic genes (12).

Constitutive MyD88-dependent TLR signals provide beneficial, noninflammatory signals (2). These signals can also trigger spontaneous inflammation. Thus, a major issue arises as to how homeostatic TLR signals are distinguished from inflammatory TLR signals. One potential mechanism for distinguishing these TLR signals may be related to recent discoveries that endogenous proteins such as IL-1R–associated kinase M (IRAK-M), ST2, and single Ig and TIR domain (SIGIRR) can restrict TLR signals (13–18). These proteins can restrict the duration and/or intensity of TLR signals and modulate the cellular outcome of TLR signaling, thereby helping to determine whether TLR signals lead to homeostatic or inflammatory responses. Notably, mice lacking IRAK-M, ST2, and SIGIRR exhibit relatively modest inflammation and survive for longer than 9–12 mo (14, 16, 17). Suppressor of cytokine signaling (SOCS) 1 can also inhibit TLR signaling, and $SOCS\text{-}1^{-/-}$ mice exhibit severe spontaneous inflammation and lymphocyte-mediated perinatal lethality; however $SOCS\text{-}1^{-/-}$ mice are rescued by the absence of IFN-γ signaling in $SOCS\text{-}1^{-/-}$ $IFN\text{-}\gamma^{-/-}$ double-mutant mice (18, 19). Thus, it is unclear whether these proteins restrict TLR signals in unperturbed mice and whether restricting homeostatic TLR signals is important for immune homeostasis.

A20 is an inducible ubiquitin-editing enzyme that restricts both TLR- and TNF-induced responses by regulating the ubiquitylation of key signaling proteins (20, 21, 22, 23). A20-deficient ($A20^{-/-}$) mice spontaneously develop multiorgan inflammation, severe cachexia, and premature lethality that can start within 1–2 wk of age, demonstrating the potent antiinflammatory functions of this molecule (22). In addition, $A20^{-/-}$ $RAG\text{-}1^{-/-}$ double-mutant mice spontaneously develop severe inflammation, cachexia, and premature death, indicating that A20 potently regulates innate immune homeostasis in the absence of adaptive lymphocytes (22). Although A20 is critical for restricting TNF-induced NF-κB signals, both $A20^{-/-}$ $TNF^{-/-}$ and $A20^{-/-}$ $TNFR1^{-/-}$ double-mutant mice spontaneously develop inflammation, cachexia, and premature death, indicating that A20 is critical for restricting inflammatory signals independently of TNF/TNFR1 signaling (22).

A20 expression is rapidly induced in macrophages upon TLR stimulation and is required for restricting the duration of TLR-induced NF-κB signaling and the quantity of TLR-induced proinflammatory cytokines (22). Hence, A20 functions as a negative feedback regulator of exogenous TLR-induced signals. As TLR ligands from commensal microorganisms may engage host cells during homeostatic conditions, we have investigated the potential roles A20 may play in regulating homeostatic TLR signals by interbreeding $A20^{-/-}$ mice with $MyD88^{-/-}$ mice. In addition, we have questioned the role of commensal bacteria in driving spontaneous inflammation in $A20^{-/-}$ mice. Finally, we have used $A20^{-/-}$ $MyD88^{-/-}$ double-mutant mice to examine the role of A20 in regulating MyD88-independent TLR signals.

RESULTS

MyD88 deficiency prevents premature lethality and cachexia in $A20^{-/-}$ mice

As commensal microbes or endogenous ligands may engage host TLRs under basal conditions, we investigated whether TLR signals contribute to the development of spontaneous inflammation in $A20^{-/-}$ mice by genetically removing MyD88-dependent TLR signals. $A20^{-/-}$ mice were interbred with $MyD88^{-/-}$ mice and backcrossed at least five generations to C57BL/6. Remarkably, although only 30% of $A20^{-/-}$ mice survive to 8 wk of age, nearly 95% of $A20^{-/-}$ $MyD88^{-/-}$ double-mutant mice survive past this age (Fig. 1 A). This improved survival rate is similar to that of $MyD88^{-/-}$ mice. Additionally, surviving $A20^{-/-}$ $MyD88^{-/-}$ double-mutant animals do not exhibit the severe cachexia manifested by surviving $A20^{-/-}$ mice (Fig. 1 B). $A20^{-/-}$ mice weigh only ∼60% of what wild-type controls weigh, whereas $A20^{-/-}$ $MyD88^{-/-}$ mice weigh ∼90% of what $MyD88^{-/-}$ controls weigh (Fig. 1 C). These data suggest that MyD88 signals drive potent proinflammatory responses that lead to cachexia and premature death in the absence of A20.

Homeostatic MyD88-dependent signals activate myeloid cells in $A20^{-/-}$ mice

MyD88-dependent TLR signals activate myeloid cells, leading to the production of cytokines that recruit and activate other innate immune cells. $A20^{-/-}$, $A20^{-/-}$ $RAG\text{-}1^{-/-}$ double-mutant, $A20^{-/-}$ $TNF^{-/-}$ double-mutant, and $A20^{-/-}$ $TNFR1^{-/-}$ double-mutant mice all spontaneously accumulate myeloid cells in both lymphoid and nonlymphoid tissues (21, 22). To begin to examine the role of MyD88 in causing inflammation in $A20^{-/-}$ mice, we measured the spleen weights as a reflection of the cellularity of these organs. Spleen weights were dramatically increased in $A20^{-/-}$ mice when compared with wild-type or $MyD88^{-/-}$ mice (Fig. 2 A), and this splenomegaly was particularly impressive given that $A20^{-/-}$ mice were significantly smaller than the other genotypes of mice (Fig. 1 C). In contrast, the weight of spleens obtained from double-deficient $A20^{-/-}$ $MyD88^{-/-}$ mice was significantly less than that obtained from $A20^{-/-}$ mice and more closely approximated the weight of spleens obtained from wild-type and $MyD88^{-/-}$ mice (Fig. 2 A).

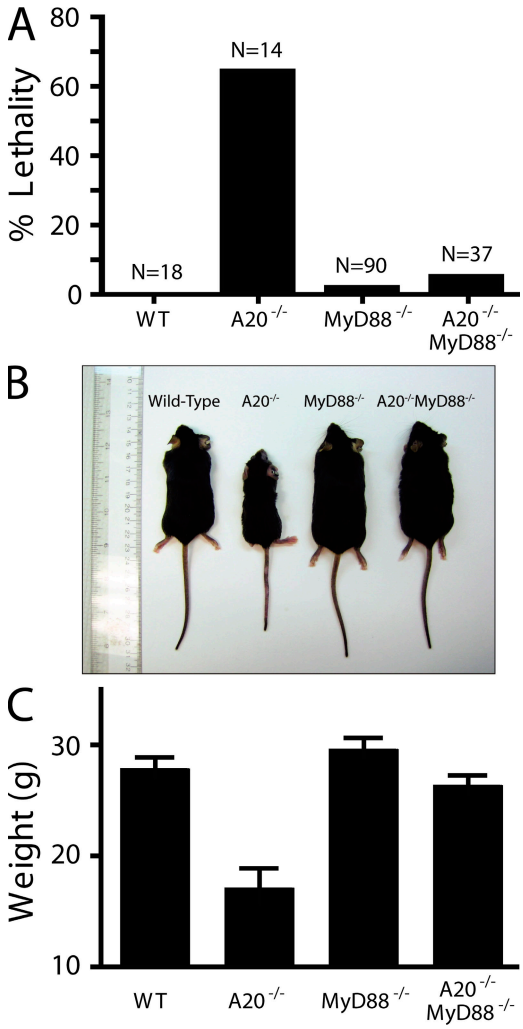

Figure 1. MyD88-dependent cachexia and lethality in A20$^{-/-}$ mice. (A) Survival of mice from the indicated genotypes at 8 wk of age (WT, A20$^{+/-}$ MyD88$^{+/-}$; A20$^{-/-}$, A20$^{-/-}$ MyD88$^{+/-}$; MyD88$^{-/-}$, A20$^{+/-}$ MyD88$^{-/-}$; and A20$^{-/-}$ MyD88$^{-/-}$). The percentage of mice in each cohort that dies before 8 wk of age is indicated by the column heights. Total numbers of mice in each cohort are indicated above each column. (B) Representative 3-mo-old mice from the indicated genotypes. Note the cachexia of the A20$^{-/-}$ but not the A20$^{-/-}$ MyD88$^{-/-}$ mouse. (C) Weight of surviving mice. Graph represents mean body weights of 10–14-wk-old mice from the indicated genotypes. Error bars represent standard deviations. Data are representative of at least five mice from each genotype.

To further examine the cellular nature of MyD88-dependent inflammation in A20$^{-/-}$ mice, we performed flow cytometric analyses of tissues from these wild-type, A20$^{-/-}$, MyD88$^{-/-}$, and A20$^{-/-}$ MyD88$^{-/-}$ mice. These studies revealed that significantly greater numbers and percentages of myeloid (Mac1^{+} Gr1^{+}) cells accumulate spontaneously in spleens of A20$^{-/-}$ mice when compared with wild-type mice, whereas the numbers of these cells obtained from A20$^{-/-}$ MyD88$^{-/-}$ mice were significantly less than those obtained from A20$^{-/-}$ mice and more closely approximated the numbers obtained from wild-type and MyD88$^{-/-}$ mice (Fig. 2, B and C). Myeloid cells were selectively expanded in tissues of A20$^{-/-}$ mice at the cost of other cells, as the percentage of Mac1^{+} Gr1^{+} cells was increased when compared with wild-type or MyD88$^{-/-}$ mice (Fig. 2 C). This expansion was also largely (but not completely) ameliorated in A20$^{-/-}$ MyD88$^{-/-}$ mice. To assess the functional activation of myeloid cells such as macrophages, we measured serum levels of IL-6 in these mice. Serum IL-6 levels were dramatically elevated in A20$^{-/-}$ mice, as compared with MyD88$^{-/-}$ or wild-type mice, whereas A20$^{-/-}$ MyD88$^{-/-}$ mice had undetectable levels of IL-6 (Fig. 2 D). These findings indicate that A20 prevents spontaneous activation and recruitment of innate immune cells in mice by restricting homeostatic MyD88-dependent signals.

Homeostatic MyD88-dependent signals activate T cells in A20$^{-/-}$ mice

TLR-dependent signals play important roles in inducing adaptive immune response during microbial infections (24, 25). For example, MyD88-dependent signals on antigen-presenting cells support the activation and expansion of T cells. To determine whether basal MyD88-dependent signals cause spontaneous activation and expansion of T cells in unperturbed A20$^{-/-}$ mice, we examined the number and activation state of T cells from A20$^{-/-}$, A20$^{-/-}$ MyD88$^{-/-}$, and control mice. Significantly greater percentages (and total numbers) of activated, memory phenotype (CD44^{Hi} CD62L^{Lo}) T cells were present in lymph nodes and spleens of A20$^{-/-}$ mice when compared with wild-type mice (Fig. 3 A and not depicted). In contrast, T cells from A20$^{-/-}$ MyD88$^{-/-}$ double-mutant mice were less activated than those from A20$^{-/-}$ mice and were more comparable to wild-type and MyD88$^{-/-}$ mice. This reduction in spontaneous T cell activation was observed in both CD4^{+} and CD8^{+} T cell populations (Fig. 3, B and C). This finding suggests that homeostatic MyD88-dependent signals cause T cell activation in the absence of A20.

Homeostatic MyD88-dependent signals in radiation sensitive hematopoietic cells drive myeloid cell activation in A20$^{-/-}$ mice

Hematopoietically derived cells such as macrophages and dendritic cells are able to sample surrounding microflora and transmit basal proinflammatory signals. In addition, A20 and MyD88 are both expressed in epithelial cells and stromal cells, which can also respond to TLR ligands. Thus, A20's role in restricting MyD88-dependent signals could involve signals on either hematopoietic cells, stromal cells, or both. To isolate the potential role of A20 in regulating MyD88 signaling in hematopoietic cells, Ly5.2 C57BL/6 mice were lethally irradiated and reconstituted with bone marrow hematopoietic stem cells (HSCs) from either wild-type, A20$^{-/-}$, MyD88$^{+/+}$, MyD88$^{-/-}$, or A20$^{-/-}$ MyD88$^{-/-}$ mice. Flow cytometric analyses of tissues from these chimera were then performed 6 wk after reconstitution. Similar to our findings with intact mice, spleens from radiation chimera reconstituted with A20$^{-/-}$ HSCs contained increased numbers of various myeloid cell types when compared with chimera reconstituted with wild-type HSCs (Fig. 4 A).

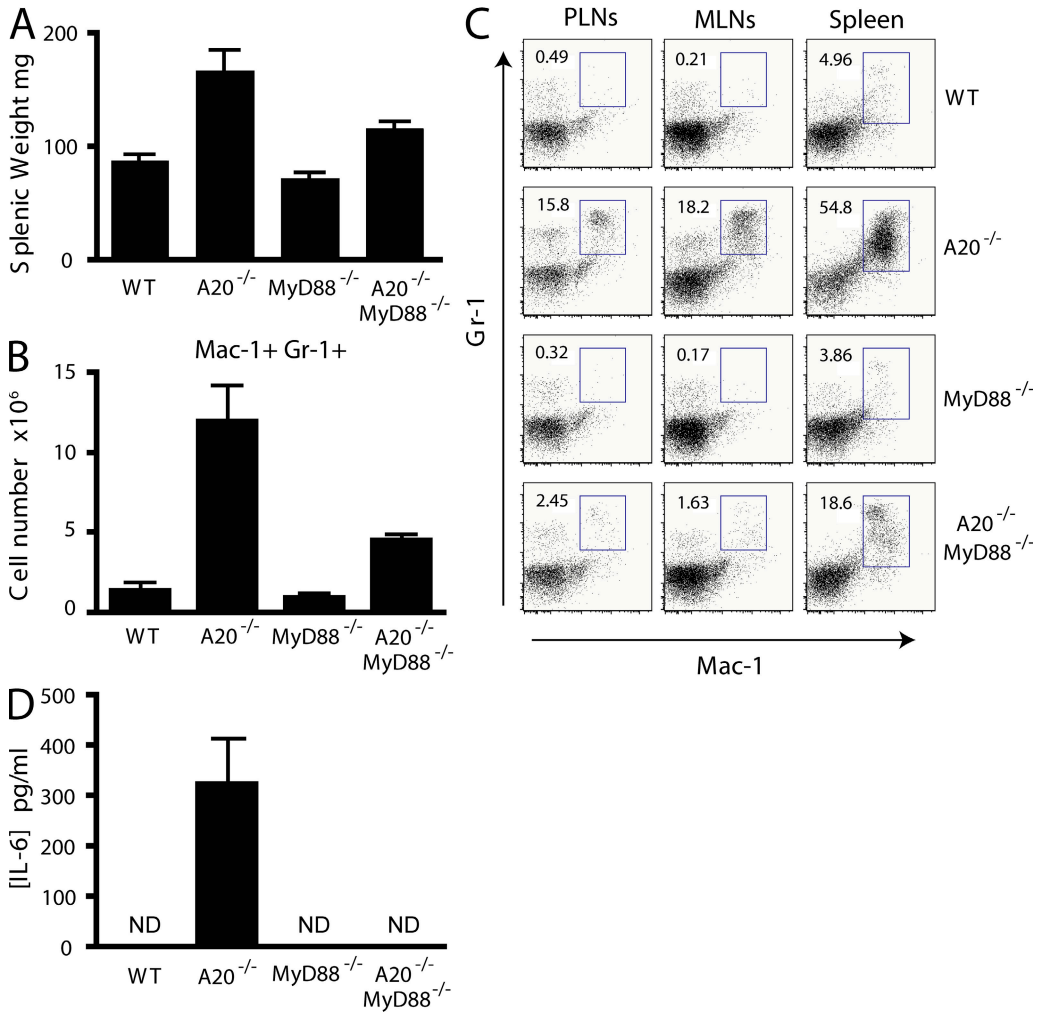

Figure 2. Reduced myeloid accumulation and splenomegaly in A20$^{-/-}$ MyD88$^{-/-}$ mice. (A) Spleen weights from 6–8-wk-old mice of the indicated genotypes. (B) Total numbers of Mac1$^+$ Gr1$^+$ myeloid cells (activated macrophages and granulocytes) from spleens of mice of the indicated genotypes. (C) Representative flow cytometric analysis of Mac-1$^+$ Gr-1$^+$ myeloid cells from peripheral and mesenteric lymph nodes and spleens from mice of the indicated genotypes. Note the decreased frequency and numbers of myeloid cells in lymphoid organs from A20$^{-/-}$ MyD88$^{-/-}$ mice compared with A20$^{-/-}$ mice. Numbers indicate the percentage of live Mac-1$^+$ Gr-1$^+$ splenocytes within the indicated gates. (D) ELISA analyses of IL-6 levels in serum from mice of the indicated genotypes. Error bars represent standard deviations. Data are representative of at least five mice from each genotype.

The myeloid cells that expand in A20$^{-/-}$ HSC-reconstituted chimera spleens include various myeloid populations such as macrophages (Mac-1$^+$, F480$^+$, and Siglec F$^-$), neutrophils (Mac-1$^+$, Gr-1$^+$, F480$^-$, and Siglec F$^-$), and eosinophils (Mac-1$^+$, Siglec F$^+$, and SSC^{Hi}) without any particular skewing toward particular subsets (Fig. 4 A). The absolute numbers of these populations were generally reduced in A20$^{-/-}$ MyD88$^{-/-}$ HSC-reconstituted chimera compared with A20$^{-/-}$ HSC-reconstituted chimera, although some of these reductions were less dramatic than the differences observed in intact A20$^{-/-}$ MyD88$^{+/+}$ and A20$^{-/-}$ MyD88$^{-/-}$ mice (Figs. 2 and 4 A). To further characterize the nature of the spontaneous inflammation caused by A20$^{-/-}$ hematopoietic cells in these chimera, we analyzed splenic production of cytokines. These studies revealed that spleens from A20$^{-/-}$ HSC-reconstituted chimera produced elevated levels of TNF and IL-1β (Fig. 4 B). These indicators of spontaneous inflammation were absent in A20$^{-/-}$ MyD88$^{-/-}$ HSC-reconstituted chimera (Fig. 4 B). As IL-10–deficient mice have recently been described to develop spontaneous colitis that resolves in the absence of MyD88 signals (3), we examined whether A20$^{-/-}$ HSC-reconstituted chimera were IL-10 deficient. A20$^{-/-}$ mice expressed elevated levels of IL-10, suggesting that IL-10 deficiency does not contribute to spontaneous inflammation in A20$^{-/-}$ mice (Fig. 4 B). A20$^{-/-}$ HSC-reconstituted chimera also expressed normal levels of IL-2 and possessed normal numbers of functional regulatory T cells (Fig. 4 B and not depicted). Thus, IL-2 deficiency is also unlikely to explain the spontaneous inflammation in A20$^{-/-}$ mice. Finally, A20$^{-/-}$ HSC-reconstituted chimera expressed elevated levels of IL-13 as well as the prototypical Th1 cytokines TNF and IFN-γ (Fig. 4 B and not depicted). Hence, no gross evidence of Th1 or Th2 skewing is evident in these mice.

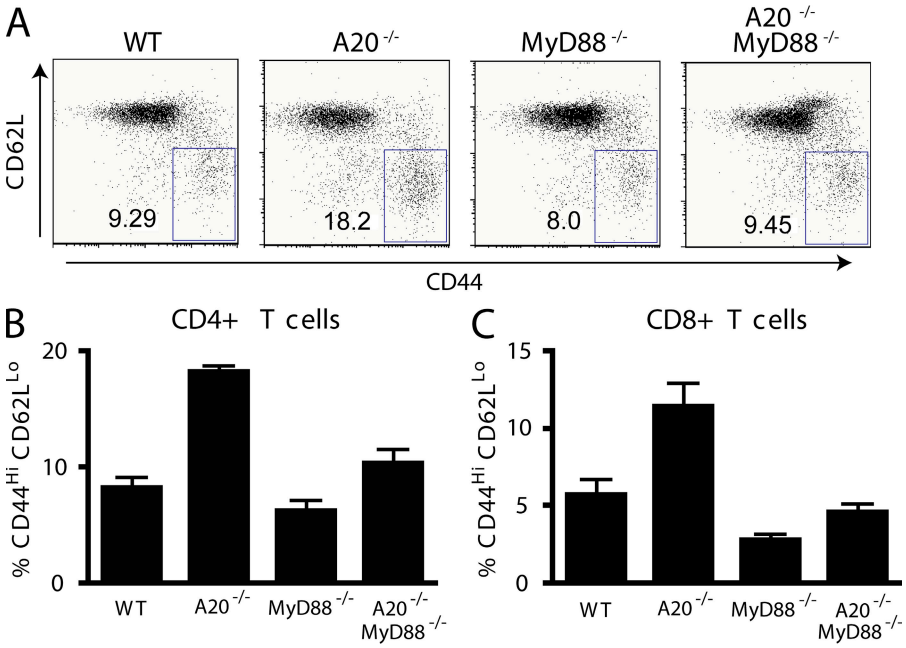

Figure 3. MyD88 dependence of T cell hyperactivation in A20$^{-/-}$ mice. (A) Flow cytometric analyses of T cell phenotypes from peripheral lymph nodes from 5–6-wk-old mice of the indicated genotypes. Representative FACS plots of CD4$^+$ T cells. The numbers represent the percentages of CD4$^+$ T cells that are CD44^{Hi} and CD62L^{Lo} (boxed gates), indicating an effector/memory T cell phenotype. Note the increased frequency of activated CD4$^+$ T cells in A20$^{-/-}$ animals, and the reduced percentages of activated T cells in A20$^{-/-}$ MyD88$^{-/-}$ mice. (B) Quantitation of activated CD4$^+$ (CD44^{Hi} CD62L^{Lo}) T cells. (C) Quantitation of activated CD8$^+$ T cells. Error bars represent standard deviations. Data are representative of at least three mice per genotype.

Collectively, these data suggest that homeostatic MyD88 signals in hematopoietic cells drive a broad spectrum of spontaneous proinflammatory pathways in the absence of A20.

Commensal bacteria stimulate homeostatic MyD88-dependent signals

Homeostatic MyD88-dependent signals may be derived from host molecules or from commensal microbes that express TLR ligands and are in constant contact with host cells. By far, the most abundant source of commensal microbes is the intestinal lumen. Thus, to determine whether commensal intestinal microbes stimulate the homeostatic MyD88-dependent signals that drive inflammation in A20$^{-/-}$ mice, we first generated radiation chimera using HSCs from A20$^{+/+}$ and A20$^{-/-}$ bone marrows. 2 wk after irradiation, we treated these chimera with oral broad spectrum antibiotics previously shown to markedly reduce the number of intestinal bacteria (vancomycin, neomycin, metronidazole, ampicillin, and trimethoprim-sulfamethoxazole). After 3 wk of treatment with this antibiotic cocktail (or with trimethoprim-sulfamethoxazole alone as a control), chimeric mice were analyzed for the numbers of intestinal bacteria as well as for evidence of spontaneous inflammation. Chimera reconstituted with A20$^{-/-}$ HSCs developed spontaneous cachexia and lost weight when compared with chimera reconstituted with wild-type HSCs (Fig. 5 A). These results suggest that A20$^{-/-}$ hematopoietic cells recapitulate the spontaneous inflammation observed in intact A20$^{-/-}$ mice. Chimera treated with the cocktail of broad spectrum antibiotics possessed several orders of magnitude fewer intestinal bacteria (not depicted). In contrast with A20$^{-/-}$ HSC-reconstituted chimera treated with trimethprim-sulfamethoxazole alone, A20$^{-/-}$ HSC-reconstituted chimera treated with the cocktail of broad spectrum antibiotics maintained their weight (Fig. 5 A). Thus, antibiotic treatment prevents cachexia caused by A20 deficiency. Large numbers of Mac1$^+$ Gr1$^+$ myeloid cells spontaneously accumulated in the spleens of A20$^{-/-}$ HSC-reconstituted chimera but not in spleens from antibiotic-treated A20$^{-/-}$ HSC-reconstituted chimera (Fig. 5 B). Finally, spleens from A20$^{-/-}$ HSC-reconstituted chimera spontaneous produced elevated levels of IL-6 and TNF messenger RNAs (mRNAs) compared with spleens from wild-type HSC-reconstituted chimera (Fig. 5 C). These indicators of inflammation were ameliorated in A20$^{-/-}$ HSC-reconstituted chimera treated with broad spectrum antibiotics (Fig. 5 C). Collectively, these results indicate that commensal intestinal bacteria drive spontaneous cachexia and myeloid inflammation via MyD88 signals in the absence of A20.

TRIF-dependent TLR signals are restricted by A20

In the absence of the TLR adaptor MyD88, TLR3 and TLR4 signal through an alternate adaptor protein, TRIF. TRIF-dependent responses lead to the production of type I IFNs (IFN-α and IFN-β) and are critical for productive antiviral immunity (10, 11). We thus asked whether A20 was physiologically required for restricting TRIF-dependent TLR responses. To examine this question, we injected LPS intraperitoneally

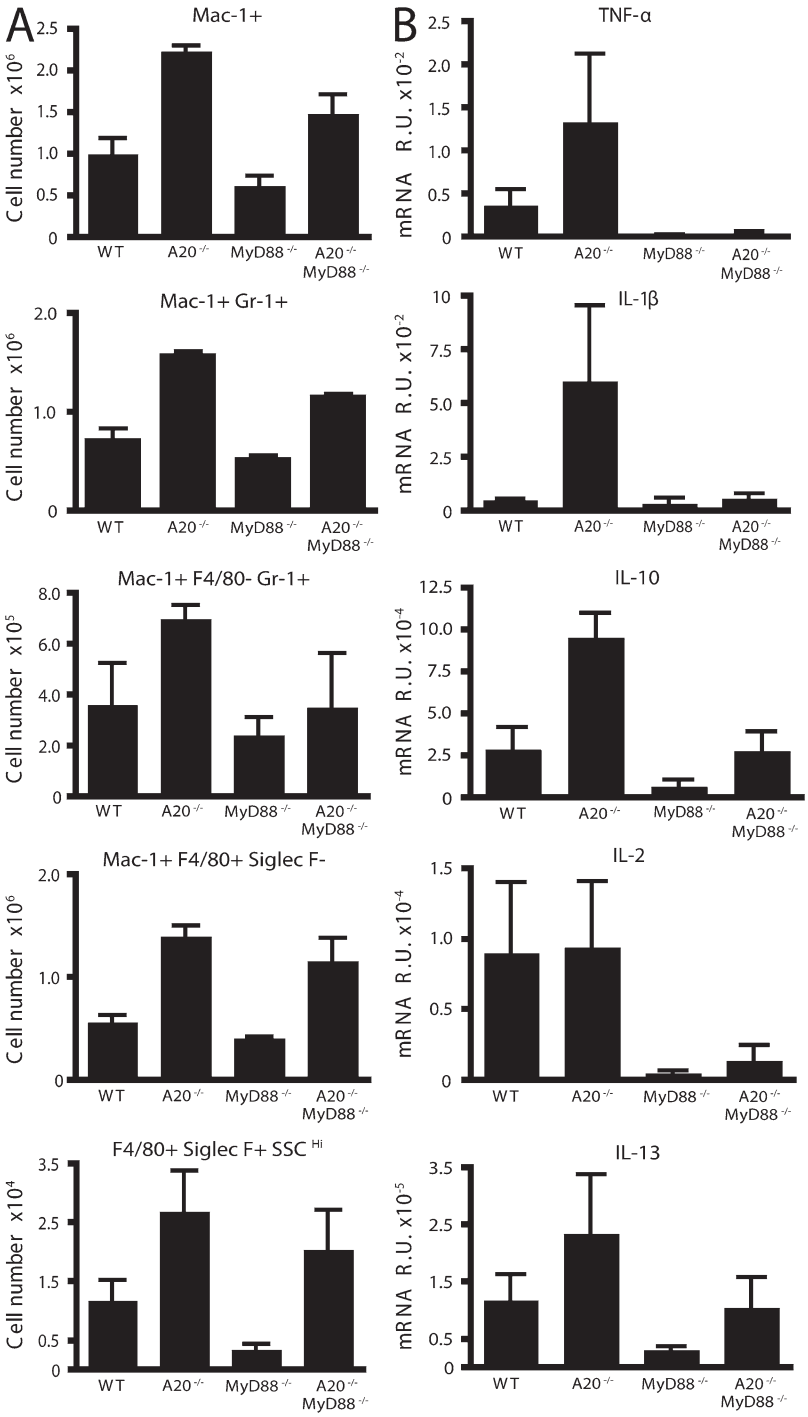

Figure 4. A20 expression in hematopoietic cells restricts MyD88-driven spontaneous inflammation in radiation chimera. (A) Flow cytometric analyses of chimeric mice generated by transfer of $A20^{+/-}$ $MyD88^{+/-}$, $A20^{-/-}$ $MyD88^{+/+}$, $A20^{+/+}$ $MyD88^{-/-}$, or $A20^{-/-}$ $MyD8^{-/-}$ bone marrow HSCs into lethally irradiated C57BL/6J mice. 6 wk after reconstitution, spleens from chimeric mice were analyzed by flow cytometry for the number of the indicated myeloid cell types ($Mac1^+$ $Gr1^+$, activated macrophages and neutrophils; $Mac1^+$ $F4/80^-$ $Gr1^+$, neutrophils; $Mac1^+$ $F4/80^+$ Siglec F^-, macrophages; and $F4/80^+$ Siglec F^+ SSC^{Hi}, eosinophils). The numbers of Mac-1^+ , Mac-1^+ Gr-1^+, and Mac-1^+ $F4/80^-$ Gr-1^+ cells were statistically different ($P < 0.05$) between $A20^{-/-}$ and $A20^{-/-}$ $MyD88^{-/-}$ mice. (B) Quantitative real-time PCR analyses of mRNA levels of the indicated cytokines in spleens from chimeric mice. Splenic expression levels of the indicated cytokines are shown in R.U. for the chimeric mice described in A. All cytokine mRNA levels were normalized to β-actin mRNA. The levels of cytokines were statistically different between $A20^{-/-}$ and $A20^{-/-}$ $MyD88^{-/-}$ mice for all cytokines. Error bars indicate standard deviations. Graphs display results from at least three independent mice per genotype.

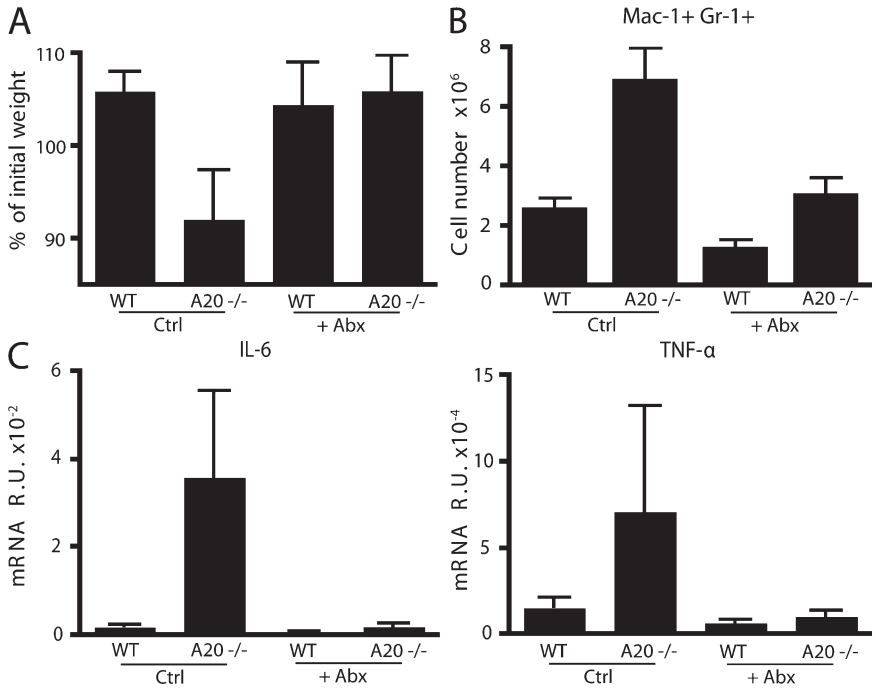

Figure 5. Depletion of commensals with broad-spectrum antibiotics diminishes inflammation driven by A20$^{-/-}$ hematopoietic cells. Chimeric mice were generated from transfer of A20$^{+/+}$ (WT) or A20$^{-/-}$ Ly5.1^{+} bone marrow HSCs into sublethally irradiated congenic Ly5.2^{+} C57BL/6J mice. 2 wk after irradiation, animals were given 0.5 gram per liter of vancomycin, 1 gram per liter of ampicillin, 1 gram per liter of neomycin, 1 gram per liter of metronidazole, and trimethoprim-sulfamethoxazole in drinking water for 3–4 wk (+Abx) or maintained on trimethoprim-sulfamethoxazole (Ctrl) for the same period. (A) The percent weight change of chimeric mice reconstituted with HSCs of the indicated genotypes and treated with either broad spectrum (+Abx) or control antibiotics (Ctrl). The percent change was calculated by dividing the weight of each mouse on the day of death/analysis by the weight on the day of irradiation and HSC reconstitution. (B) Flow cytometric analyses of Ly5.1^{+} Mac1^{+} Gr1^{+} cells from spleens of chimeric mice. (C) Quantitative real-time PCR analysis of mRNA levels of IL-6 and TNF in spleens of chimeric mice. Note that A20$^{-/-}$ HSC-reconstituted chimera spontaneously lose weight, accumulate myeloid cells, and express higher levels of splenic IL-6 and TNF than A20$^{+/+}$ HSC-reconstituted chimera, whereas treatment of A20$^{-/-}$ HSC-reconstituted chimera with broad spectrum antibiotics prevents these signs of inflammation. Error bars represent standard deviations. Data are representative of five mice.

into either A20$^{-/-}$ MyD88$^{-/-}$ or MyD88$^{-/-}$ HSC-reconstituted chimeric mice and measured the resulting TRIF-dependent inflammatory response. We first measured the production of IFN-β and monocyte chemoattractant protein (MCP) 1, two TRIF-dependent proinflammatory cytokines that are produced by macrophages and dendritic cells. Quantitative real-time PCR analysis of splenocytes from these mice revealed that IFN-β and MCP-1 expression are induced by LPS to a greater degree in A20$^{-/-}$ MyD88$^{-/-}$ HSC-reconstituted chimera than in MyD88$^{-/-}$ HSC-reconstituted chimera (Fig. 6 A). To assess the role of A20 in regulating MyD88-independent recruitment of granulocytes to LPS, we quantitated the number of Mac-1^{+} Gr-1^{+} F4/80^{-} cells (neutrophils) recruited to the peritoneal cavity 2 h after LPS injection. These experiments indicated that far greater numbers of these cells were obtained from the peritoneal lavage of LPS-stimulated A20$^{-/-}$ MyD88$^{-/-}$ HSC-reconstituted chimera than from MyD88$^{-/-}$ HSC-reconstituted chimera (Fig. 6 B). We also measured the production of MCP-1 protein in peritoneal lavages from these mice by ELISA and found that MCP-1 protein was produced at higher levels in A20$^{-/-}$ MyD88$^{-/-}$ HSC-reconstituted chimera than in MyD88$^{-/-}$ HSC-reconstituted chimera (Fig. 6 C). Finally, IFN-β stimulates IL-15 and IL-15Rα production, leading to NK cell activation in early antiviral immunity. Soluble IL-15Rα is released into the serum during this process (unpublished data). We thus measured serum IL-15Rα protein levels in LPS-stimulated chimeric mice by ELISA, and these assays showed that higher levels of soluble IL-15Rα were present in LPS-stimulated A20$^{-/-}$ MyD88$^{-/-}$ chimera than in LPS-stimulated MyD88$^{-/-}$ chimera (Fig. 6 D). Collectively, these findings indicate that A20 is physiologically required for restricting acute, MyD88-independent, TRIF-dependent proinflammatory signals in vivo.

A20 regulates TRIF-dependent TLR-induced NF-κB signaling but not IRF3 signaling

TRIF-dependent TLR signals involve both NF-κB and IRF3-dependent signals (26, 27). To determine how A20 regulates TRIF-dependent TLR responses, we first interbred A20$^{-/-}$ MyD88$^{-/-}$ mice with TNF$^{-/-}$ mice. The resulting triple-mutant mice allowed us to evaluate TRIF-dependent TLR signals in the absence of secondary TNF signaling. We then prepared bone marrow–derived macrophages (BMDMs) from these TNF$^{-/-}$ MyD88$^{-/-}$ and A20$^{-/-}$ TNF$^{-/-}$ MyD88$^{-/-}$ mice.

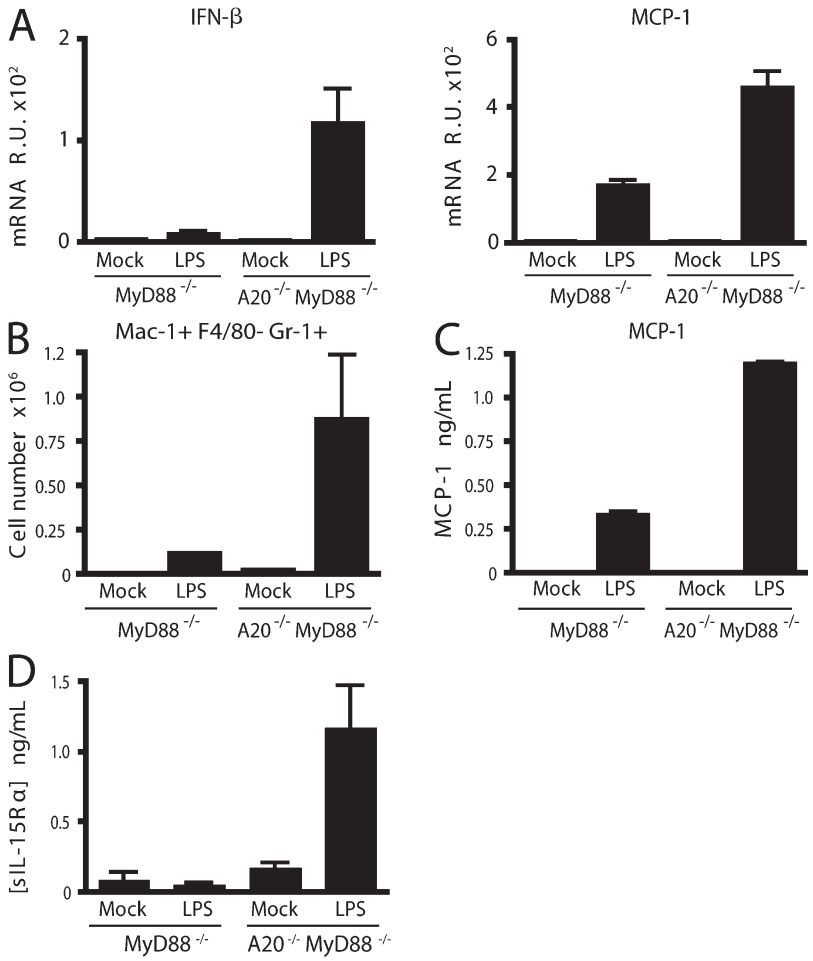

Figure 6. A20 expression in hematopoietic cells restricts TRIF-dependent LPS responses in vivo. Chimeric mice were generated using HSCs of the indicated genotypes and lethally irradiated C57BL/6J mice. 6 wk after reconstitution, chimeric mice were injected with 100 µg LPS or PBS (mock) intraperitoneally and killed after 2 h. (A) Real-time PCR analyses of IFN-β and MCP-1 mRNA levels in splenocytes from the indicated mice. mRNA levels were normalized to GAPDH mRNA and expressed as R.U. (B) Flow cytometric analyses of the number of $Mac1^+$ $Gr1^+$ $F4/80^-$ neutrophils recruited to the peritoneal cavities of the indicated mice. Absolute numbers of neutrophils obtained in 5 ml of peritoneal lavage are shown. (C) ELISA determination of levels of MCP-1 protein obtained in peritoneal lavages of mice of the indicated genotypes. (D) ELISA determination of soluble IL-15Rα levels measured in the serum of the indicated mice. Error bars represent standard deviations. Data are representative of three mice in each treatment group.

Comparable numbers and phenotypes of these two types of BMDMs were obtained after 6 d of culture in MCSF-supplemented media (not depicted). We then tested the responses of these cells to LPS or poly-inosine:cytosine (poly (I:C)), ligands for TLR4 and TLR3, respectively. After either of these stimuli, $A20^{-/-}$ $TNF^{-/-}$ $MyD88^{-/-}$ BMDMs secreted greater amounts of IFN-β than $TNF^{-/-}$ $MyD88^{-/-}$ BMDMs (Fig. 7 A and not depicted). Thus, A20 appears to be directly required for restricting TRIF-dependent TLR responses independently of TNF signaling.

The production of IFN-β is dependent on both NF-κB as well as IRF3 signaling, as the IFN-β promoter contains binding elements for both these transcription factors. To further understand the mechanism by which A20 restricts TRIF-dependent TLR signaling, we stimulated $A20^{-/-}$ $TNF^{-/-}$ $MyD88^{-/-}$ and $TNF^{-/-}$ $MyD88^{-/-}$ BMDMs with LPS, prepared whole-cell lysates at various time points, and analyzed these lysates for the expression of IκBα and phospho-IκBα by immunoblotting. When compared with $TNF^{-/-}$ $MyD88^{-/-}$ BMDMs, $A20^{-/-}$ $TNF^{-/-}$ $MyD88^{-/-}$ cells exhibited prolonged expression of phospho-IκBα and delayed recovery of IκBα, indicating that A20 is required for restricting TRIF-dependent NF-κB signaling (Fig. 7 B).

In addition to activating NF-κB signaling, TLR3- and TLR4-induced activation of TRIF also causes IRF3 phosphorylation, which in turn leads to its dimerization, nuclear translocation, and stimulation of IFN-α/β gene transcription (12). $TNF^{-/-}$ $MyD88^{-/-}$ and $A20^{-/-}$ $TNF^{-/-}$ $MyD88^{-/-}$ BMDMs were stimulated with LPS for various time periods. Phospho-IRF3 levels were then measured by immunoblotting of nuclear protein extracts. Surprisingly, $TNF^{-/-}$ $MyD88^{-/-}$ and $A20^{-/-}$ $TNF^{-/-}$ $MyD88^{-/-}$ BMDMs activated phospho-IRF3 with similar kinetics and intensity (Fig. 7 C). Thus, A20 is required for restricting TRIF-dependent NF-κB signaling but not

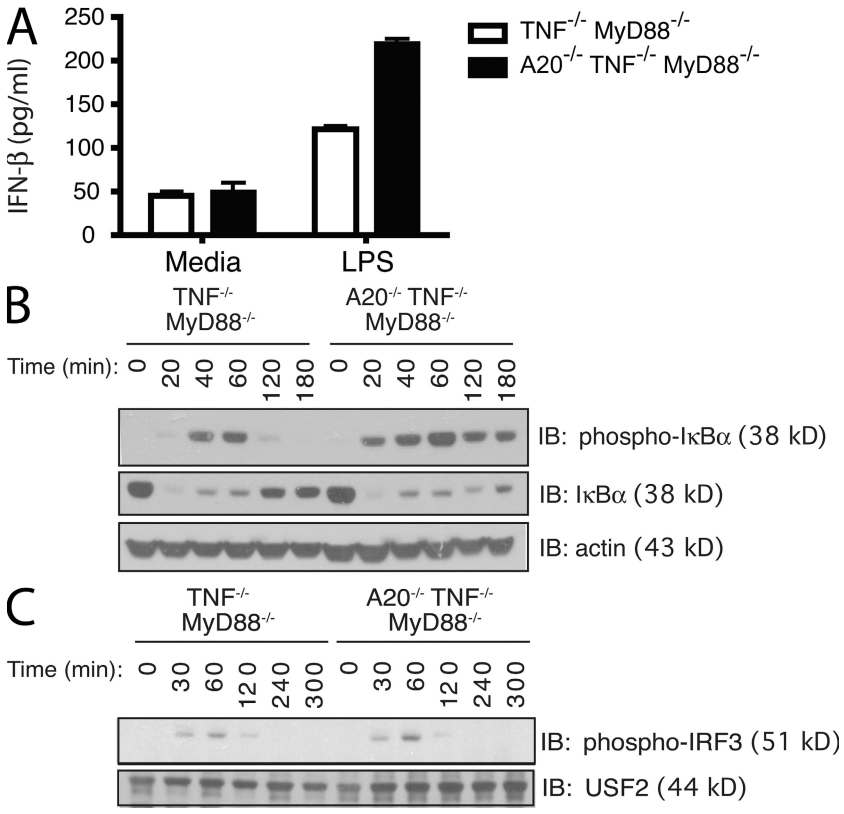

Figure 7. A20 is critical for directly restricting MyD88-independent LPS responses. (A) ELISA analysis of IFN-β secretion by LPS-stimulated BMDMs. $TNF^{-/-}$ $MyD88^{-/-}$ and $A20^{-/-}$ $TNF^{-/-}$ $MyD88^{-/-}$ BMDMs were stimulated for 24 h with LPS, after which supernatants were harvested for ELISA. (B) Immunoblotting analyses of phospho-IκBα and IκBα protein expression by LSP-stimulated BMDMs. $TNF^{-/-}$ $MyD88^{-/-}$ and $A20^{-/-}$ $TNF^{-/-}$ $MyD88^{-/-}$ BMDMs were stimulated with LPS for the indicated times, after which cells were lysed for immunoblotting analyses for the indicated proteins. Actin protein levels are shown as a loading control. (C) Immunoblotting analyses of nuclear lysates for phospho-IRF3 protein expression by LPS-stimulated BMDMs. Nuclear USF2 protein levels are shown as a control. The black line indicates that intervening lanes have been spliced out. Data are representative of at least three experiments.

TRIF-dependent IRF3 signaling. Moreover, these data suggest that increased IFN-β production from $A20^{-/-}$ $TNF^{-/-}$ $MyD88^{-/-}$ BMDMs, when compared with $A20^{+/+}$ $TNF^{-/-}$ $MyD88^{-/-}$ BMDMs, is caused by increased NF-κB signaling and not increased IRF3 signaling.

A20 is essential for restricting TLR-induced TNF receptor–associated factor (TRAF) 6 ubiquitination

Our previous studies showed that A20 restricts TLR-induced NF-κB signaling (22). Our current studies indicate that A20 regulates TRIF-dependent NF-κB signaling but not IRF3 signaling. Collectively, these data suggest that the major function of A20 in TLR signaling is to directly regulate a signaling event that is common to MyD88- and TRIF-dependent NF-κB signaling and that is not shared by TRIF-dependent IRF3 signaling. TRAF6 is an E3 ligase that is involved in both MyD88- and TRIF-dependent NF-κB signaling (28–30). Upon stimulation with TLR ligands, TRAF6 is recruited to the TLR in both MyD88-dependent and -independent signaling pathways. TRAF6 autoligates lysine-63 ubiquitin chains upon TLR or IL-1R stimulation to activate NF-κB, and our previous studies showed that A20 is able to use its OTU protease domain to deubiquitylate TRAF6 (22, 30). Thus, TRAF6 may be a physiological target for A20 during TLR signaling. To directly determine if A20 is essential for regulating TRAF6 ubiquitylation during TLR stimulation, $A20^{+/+}$ and $A20^{-/-}$ BMDMs were stimulated with LPS for various periods of time, after which cell lysates were analyzed for their expression of ubiquitylated TRAF6. Endogenous TRAF6 is ubiquitylated after 20 min of LPS stimulation (Fig. 8). Importantly, whereas TRAF6 ubiquitylation is transiently induced in $A20^{+/+}$ cells, declining after 40 min, TRAF6 ubiquitylation is prolonged to 40 and 60 min in $A20^{-/-}$ cells (Fig. 8). As these lysates were boiled in 1% SDS before immunoprecipitation of TRAF6, the ubiquitylated proteins we observe are likely to be predominantly ubiquitylated TRAF6 rather than noncovalently associated proteins. This finding indicates that A20 is essential for restricting endogenous TRAF6 ubiquitylation after TLR stimulation.

DISCUSSION

Our studies have shed new light on the importance and regulation of homeostatic TLR signals. Recent studies have indicated that homeostatic TLR signals may be chronically triggered by PAMPs from microbes at mucosal surfaces such as

the intestinal epithelium. MyD88-dependent TLR signals may be beneficial for intestinal homeostasis under normal circumstances (2, 31). The appreciation of such homeostatic TLR signals has raised several questions, including whether homeostatic TLR signals are potentially inflammatory. Our finding that unperturbed A20$^{-/-}$ MyD88$^{-/-}$ mice are dramatically less inflamed and survive far longer than A20$^{-/-}$ MyD88$^{+/-}$ mice suggests that homeostatic TLR signals can in fact be profoundly inflammatory and rapidly lethal. We have also elucidated a new function for A20 in regulating TRIF-dependent NF-κB signals but not IRF3 signals.

The idea that homeostatic MyD88 signals can cause spontaneous inflammation is broadly consistent with recent findings that constitutive MyD88 signals drive colitis and eventual mortality in IL-10$^{-/-}$ mice (3). However, although IL-10$^{-/-}$ mice develop progressive colitis during the first 4–6 mo of life and eventually die from this disease, the majority of A20$^{-/-}$ mice die within the first 3–6 wk of life from widespread systemic inflammation and cachexia (3, 32). Thus, our findings indicate that homeostatic MyD88 signals can drive severe perinatal systemic inflammation in addition to intestinal inflammation. Moreover, although IL-10 is particularly important for restricting intestinal inflammation, A20 is critical for restricting systemic inflammation.

Although A20 prevents widespread inflammation, a major source of constitutive, proinflammatory TLR signals in A20$^{-/-}$ mice may nevertheless be intestinal commensal bacteria. We have found that the removal of many of these bacteria with antibiotics reduced systemic inflammation in chimeric mice bearing A20$^{-/-}$ hematopoietic cells. Although previous studies have shown that intestinal bacteria can drive intestinal inflammation in several models (33), our current results link these bacteria and MyD88-dependent signals to A20-mediated regulation of innate immune cells and to systemic immune activation.

The different physiological roles of IL-10 and A20 in restricting MyD88-dependent signals is likely related to the distinct biochemical functions of these immunoregulatory proteins. IL-10 triggers STAT3-mediated transcriptional inhibition of proinflammatory genes, whereas our data indicate that A20 restricts MyD88-dependent TLR signals by regulating TRAF6 ubiquitylation. Thus, the critical physiological role that A20 plays in preventing constitutive homeostatic MyD88 signals from becoming inflammatory is likely caused by A20's biochemical role in directly regulating MyD88-dependent signals.

Proteins such as A20, IRAK-M, ST2, and SIGIRR that restrict TLR signals could regulate the duration and/or intensity of TLR signals and modulate the cellular outcome of TLR signaling, thereby helping to determine whether TLR signals lead to homeostatic or inflammatory responses (14–18). Notably, although unperturbed mice lacking IRAK-M, ST2, and SIGIRR exhibit relatively modest inflammation and survive for longer than 9–12 mo of age, A20$^{-/-}$ mice typically die within the first few weeks of life (13–17). Although SOCS-1$^{-/-}$ mice exhibit perinatal lethality similar to A20$^{-/-}$ mice, SOCS-1$^{-/-}$ mice are rescued by the absence of IFN-γ signaling in SOCS-1$^{-/-}$ IFN-γ$^{-/-}$ double-mutant mice (19–21). Thus, among proteins known to directly restrict TLR signaling, A20 appears to play a more critical role in regulating homeostatic TLR-driven inflammation in vivo. There are several potential (nonmutually exclusive) reasons why A20 has a greater physiological impact on homeostatic TLR signals. First, A20 enzymatically regulates ubiquitylation of signaling proteins, thereby regulating both the activity and stability of such targets. Thus, A20 may not only deactivate signaling proteins but may also prevent further reactivation of these proteins. Second, A20 may regulate TLR signaling downstream of other known TLR regulating proteins, thus exerting a more definitive impact on the transcriptional outcome of TLR signals. Third, A20's physiological roles in restricting MyD88-dependent TLR signals may be amplified by A20's roles in regulating other non-TLR signals, e.g., TNF signals. However, marked survival differences between A20$^{-/-}$ MyD88$^{-/-}$ TNF$^{-/-}$ mice and A20$^{-/-}$ TNF$^{-/-}$ mice suggest that restricting MyD88 signals may be the dominant physiological function of A20 during homeostatic conditions. Finally, it is possible that A20 may also regulate IL-1 or IL-18 signals, which also use MyD88 (9). Although we have not yet

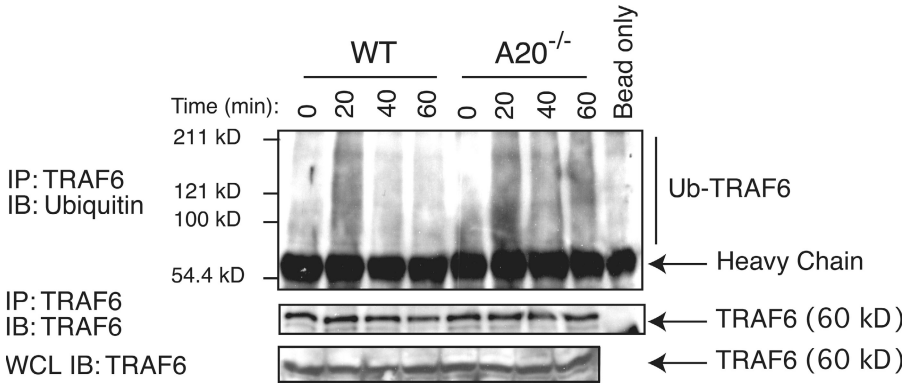

Figure 8. A20 is essential for restricting TRAF6 ubiquitylation. Immunoblotting analysis of endogenous TRAF6 ubiquitylation in LPS-stimulated BMDMs. A20$^{-/-}$ and A20$^{+/+}$ BMDMs were stimulated with LPS, and cell lysates were generated at the indicated time points. Samples were boiled in 1% SDS to disassociate noncovalent protein–protein interactions. After dilution to 0.1% SDS, TRAF6 protein was immunoprecipitated from the lysates and immunoblotted for ubiquitin. Data are representative of at least three independent experiments.

evaluated the contribution of aberrant IL-1 or IL-18 signaling to spontaneous inflammation in $A20^{-/-}$ mice, IL-1 receptor antagonist–deficient mice do not develop spontaneous inflammation within the first 4 mo of life (34). Thus, restricting basal IL-1 signals may not be critical for immune homeostasis in unperturbed mice. Collectively, A20 appears to be one of the most critical proteins for restricting homeostatic TLR signals in vivo.

Constitutive or basal MyD88-dependent signals could derive from microbial or host ligands. Our experiments with antibiotic-mediated depletion of commensal bacteria reinforce the notion that intestinal bacteria are a major source of MyD88-dependent signals triggering inflammation in unperturbed $A20^{-/-}$ mice. Collectively with previous findings that constitutive MyD88-dependent signals from luminal bacteria are required for maintaining intestinal health, the current results suggest that a moderate but not excessive magnitude of MyD88 signaling in the intestine is essential for intestinal homeostasis.

In the intestine, homeostatic TLR signals might also be distinguished from inflammatory TLR signals by microenvironment- and cell type–specific TLR signals. For example, apical TLR signals on epithelial cells might preferentially induce homeostatic signals, whereas TLR signals on dendritic cells trigger inflammation. Although we have not yet directly addressed the roles of A20 in regulating epithelial cell function, our discoveries that radiation chimera bearing $A20^{-/-}$ $MyD88^{-/-}$ hematopoietic cells exhibit less spontaneous inflammation than chimeric mice bearing $A20^{-/-}$ $MyD88^{+/+}$ cells indicates that A20-mediated restriction of homeostatic TLR signals specifically in hematopoietic cells is important for immune homeostasis. Although it is possible that TLRs on epithelial cells may also be constitutively engaged on mucosal surfaces, our results using radiation chimera indicate that engagement of TLRs on hematopoietic cells occurs in unperturbed mice and must be properly restricted to maintain immune homeostasis. Indeed, one example of how TLRs on hematopoietic cells might tonically bind PAMPs from luminal microbes is via the extrusion of dendrites by mucosal dendritic cells through epithelial tight junctions into the intestinal lumen (35–37). Future studies using gene-targeted mice bearing lineage-specific deletions of A20 should facilitate studies of A20's specific role in dendritic cells and other cell types.

The generation and characterization of $A20^{-/-}$ $MyD88^{-/-}$ mice also facilitates further studies of A20's roles in regulating additional signaling pathways. Milder but progressive spontaneous inflammation in older double-mutant $A20^{-/-}$ $MyD88^{-/-}$ mice and triple-mutant $A20^{-/-}$ $MyD88^{-/-}$ $TNF^{-/-}$ mice suggests that A20 regulates additional immune signals besides MyD88-dependent TLR and TNF signals. TRIF-dependent TLR signals may be one of these types of signals, and we have used $A20^{-/-}$ $MyD88^{-/-}$ mice to discover that A20 is also required for restricting TRIF-dependent TLR responses. We have also used $A20^{-/-}$ $MyD88^{-/-}$ and $A20^{-/-}$ $MyD88^{-/-}$ $TNF^{-/-}$ cells to decipher the biochemical mechanism by which A20 regulates TLR signaling. Specifically, both $A20^{-/-}$ $MyD88^{-/-}$ mice and BMDMs derived from these mice produce more type I IFNs than $A20^{+/-}$ $MyD88^{-/-}$ mice and BMDMs after LPS stimulation. Previous work demonstrated that TRIF associates with TANK-binding kinase 1, TRAF3, and TRAF6 during the activation of NF-κB and IRF3 signaling (10, 38). Both NF-κB and IRF3 are required for TRIF-dependent IFN transcription. Receptor-interacting protein (RIP) 1 ubiquitylation, possibly mediated by TRAF6, is also involved in TRIF-dependent NF-κB signaling (39, 40). Our data suggest that A20 restricts TRIF-dependent NF-κB signaling and not IRF3 phosphorylation. Hence, A20's nonredundant function in regulating TRIF-dependent signaling appears to be restricted to NF-κB signaling. A20 can inhibit TLR3 signals and can bind TRAF6, Nef-associated kinase/TANK-binding kinase 1, and IκB kinase ε (41–43). Thus, it is likely that A20 restricts TRIF-dependent signaling by directly regulating proteins in this signaling complex. Our data do not support the previous finding that heterologous A20 expression inhibits IRF3 dimerization, and these differences could be caused by the distinct experimental systems used (43). Collectively, our data suggest that A20 restricts TRIF-dependent IFN responses by limiting TRIF-dependent NF-κB signaling.

Previous work has shown that conjugation of K63-linked ubiquitin chains to TRAF6 is an essential step in TLR-induced NF-κB activation (30). Our earlier studies also showed that A20 is a ubiquitin-modifying enzyme that can both deconjugate ubiquitin chains and ligate ubiquitin onto target proteins such as RIP and TRAF6 (18, 23). Our current data directly demonstrate that A20 is essential for restricting endogenous TRAF6 ubiquitylation after TLR stimulation, further reinforcing this biochemical mechanism. As TRAF6 binds to both MyD88 and TRIF after TLR stimulation, TRAF6 likely activates NF-κB signals in both of these pathways. RIP1 is also involved in TRIF-dependent TLR signaling, and A20 restricts RIP1 ubiquitylation in response to TNF (39, 40). Thus, it is possible that A20 also restricts TRIF-dependent NF-κB signaling by restricting RIP1 ubiquitylation. However, RIP1 is not involved in MyD88-dependent NF-κB signaling, so it is unlikely that A20's effects on RIP1 can explain all of A20's roles in TLR signaling. In contrast, A20's restriction of TRAF6 ubiquitylation may be a common mechanism by which A20 restricts both MyD88- and TRIF-dependent NF-κB signaling.

TRAF3 has recently been implicated in TRIF-dependent signaling (44, 45). TRAF3 appears to be more important for IRF signals, whereas TRAF6 is more important for NF-κB signaling. We and others have not been able to obtain evidence that A20 binds to or modifies TRAF3 (unpublished data), and our finding that IRF3 phosphorylation occurs normally in the absence of A20 suggests that A20 may preferentially regulate TRAF6- but not TRAF3-dependent signaling. These two proteins (along with TRAF2, TRAF4, and TRAF5) share structurally homologies, including RING and Zn finger motifs that may mediate E3 ligase activity. Selective regulation of TRAF6- but not TRAF3-dependent signaling by A20 might be explained if A20 preferentially binds TRAF6 rather than TRAF3. Alternatively, although TRAF6 is modified with K63-linked polyubiquitin chains during TLR-initiated signal transduction,

it is currently unclear if TRAF3 is similarly ubiquitylated. Thus, A20 may bind K63 polyubiquitylated TRAF6, whereas TRAF3 may not undergo this type of ubiquitylation modification. In either scenario, our findings indicate that A20 is a selective regulator of TRAF6- and not TRAF3-dependent signal transduction and provides new insights into how NF-κB and IRF signaling may be discriminated and differentially regulated.

Our finding that A20$^{-/-}$ MyD88$^{-/-}$ mice virtually all survive to adulthood with modest amounts of inflammation contrasts sharply with our previous findings that A20$^{-/-}$, A20$^{-/-}$ RAG-1$^{-/-}$, A20$^{-/-}$ TNF$^{-/-}$, and A20$^{-/-}$ TNFR1$^{-/-}$ mice all spontaneously develop severe inflammation, cachexia. and premature death (18, 19). This result suggests that dysregulated homeostatic TLR signals stimulate downstream innate and adaptive immune signals in the absence of A20 (e.g., TNF, IL-12, IL-6, and chemokine production, T cell activation, B cell activation, etc). Although A20 may play multiple important roles in regulating immune cell signals, its role in restricting homeostatic TLR signals may be physiologically critical because TLR signals are situated at the apex of immune responses. Moreover, our results showing that antibiotics ameliorate inflammation in A20$^{-/-}$ chimeric mice suggest that commensal intestinal flora trigger these homeostatic MyD88-dependent TLR signals. Finally, we have established a biochemical mechanism by which A20 restricts both MyD88- and TRIF-dependent TLR signals. In summary, our findings demonstrate the profoundly proinflammatory nature of homeostatic MyD88-dependent signals and identify A20 as a critical protein that prevents homeostatic signals from becoming inflammatory. Further studies elucidating how A20 restricts different types of TLR signals should yield important insights into the complex interplay between commensal microbes and host immune cells, as well as the biochemical mechanisms by which signals triggered by microbial molecules are regulated and interpreted.

MATERIALS AND METHODS

Mice and cell preparations. The generation and characterization of A20$^{-/-}$ mice have been previously described (20). A20$^{-/-}$ mice were backcrossed for eight generations onto a C57BL/6J background. MyD88$^{-/-}$ mice were provided by S. Akira (University of Osaka, Osaka, Japan) and R. Medzhitov (Yale University, New Haven, CT) and were backcrossed for five generations onto a C57BL/6J background before being interbred with A20$^{-/-}$ mice. Chimeric mice were generated by reconstitution of lethally irradiated congenic (Ly5.2^{+}) mice with bone marrow HSCs. Flow cytometric analyses of tissues from mice were performed with a flow cytometer (LSR2; Becton Dickinson) and FlowJo software (Tree Star, Inc.). For LPS-induced peritonitis experiments, mice were injected intraperitoneally with 100 μg LPS from *Salmonella typhimurium* (Sigma-Aldrich) and killed after 2 h for real-time PCR, ELISA, and flow cytometric analyses as described. All animal experiments were approved by the Institutional Animal Care and Use Committee at the University of California, San Francisco.

BMDMs were generated in DMEM containing 10% FCS and in 10% CMG14-12–conditioned media containing MCSF. After 3 d, nonadherent cells were aspirated and adherent cells were given fresh MCSF-containing media. After an additional 3 d, BMDMs were quantitated and phenotyped by flow cytometry with antibodies specific for F4/80 (Serotec) and Mac-1 (BD Biosciences). Macrophage purity was typically 90–95%. BMDMs were allowed to adhere to tissue culture plastic overnight before stimulation.

Depletion of commensal intestinal bacteria in chimeric mice. For antibiotic-mediated depletion of commensal bacteria, chimeric mice were generated by transfer of wild-type or A20$^{-/-}$ bone marrow HSCs into sublethally (700 rads) congenic Ly5.2^{+} C57BL/6J recipient mice. All mice were given trimthoprim-sulfamethoxazole immediately after reconstitution. 2 wk after reconstitution, some mice were given 0.5 grams per liter of vancomycin hydrochloride (Novaplus), 1 gram per liter of ampicillin (Sandoz), 1 gram per liter of neomycin sulfate (Pharma-Tek), and 1 gram per liter of metronidazole (Baxter) in drinking water. After 3–4 wk, mice were killed and analyzed by flow cytometry. To quantitate colonic microflora, fecal matter was removed from colons, weighed, and homogenized in luria broth at 0.1 g/ml before culturing on LB-agar plates.

TLR ligands and ELISAs. LPS from *S. typhimurium* and poly (I:C) (GE Healthcare) were used at concentrations of 1 μg/ml and 50 ng/ml, respectively. BMDMs were stimulated with either LPS or poly (I:C) for 24 h, and culture supernatants were assayed by ELISA for IFN-β (PBL Biomedical Laboratories). Peritoneal lavages from LPS-stimulated mice were assayed by ELISA for MCP-1 secretion (BD Biosciences), and sera from these mice were assayed by ELISA for soluble IL-15Rα (Duoset; R&D Systems).

RNA isolation and quantitative PCR analyses. RNA was isolated from spleens using extraction of homogenized tissue (RNeasy Mini Kit; QIAGEN). RNA was treated with Rnase-free DNase (QIAGEN) to eliminate contaminating genomic DNA and quantified using a spectrophotometer (ND-1000; Nanodrop). Complementary DNA was generated using an RT kit (QuantiTect; QIAGEN), and real-time quantitative PCR was performed using an SYBR green PCR kit (QuantiTect; QIAGEN). The following gene-specific primers were used for quantitating TNF-α (sense, 5′-TGGCCTCCCTCTCATCAGTT-3′; antisense, 5′-TCCTCCACTTGGTGGTTTGC-3′), IL-1β (sense, 5′-CCGTGGACCTTCCAGGATGA-3′; antisense, 5′-GGGAACGTCACACACCAGCA-3′), IL-10 (sense, 5′-TGAATTCCCTGGGTGAGAAG-3′; antisense, 5′-CTCTTCACCTGCTCCACTGC-3′), IL-2 (sense, 5′-AAAAGCTTTCAATTGGAAGATGCTG-3′; antisense, 5′-TTGAGGGCTTGTTGAGATGA-3′), IL-13 (sense, 5′-GGAGCTGAGCAACATCACACA-3′; antisense, 5′-TTGAGGGCTTGTTGAGATGA-3′), β-actin (sense, 5′-AAGTGTGACGTTGACATCCGTAA-3′; antisense, 5′-TGCCTG GGTACATGGTGGTA-3′), MCP-1 (sense, 5′-CCCAATGAGTAGGCTGGAGA-3′; antisense, 5′-TCTGGACCCATTCCTTCTTG-3′), IFN-β (sense, 5′-CAGCTCCAAGAAAGGACGAAC-3′; antisense, 5′-GGCAGTGTAACTCTTCTGCAT-3′), and GAPDH (sense, 5′-AACGGGAAGCCCATCACCATCTT-3′; antisense, 5′-GCCCTTCCACAATGCCAAAGTT-3′).

Real-time PCR was performed and analyzed (ABI 7300; Applied Biosystems). mRNA relative units (R.U.) were calculated as $2^{n-(Ct[gene\ of\ interest]-Ct[control])}$, as previously described (46).

Immunoblotting and immunoprecipitations. For in vitro TLR signaling experiments, BMDMs were stimulated for the periods of time indicated in the figures with 1 μg/ml LPS, washed in PBS, and lysed for 20 min at 4°C in RIPA lysis buffer (1× PBS, 20 mM β-glycerophosphate, 1 mM Na-orthovanadate, and complete protease inhibitor cocktail; Roche) and sonicated. Lysates were cleared by centrifugation at 14,000 *g* for 20 min at 4°C, and supernatants were removed and boiled in Laemmli buffer for immunoblot analysis of IκBα, phospho-IκBα, or phospho-IRF3 (Cell Signaling Technology). For endogenous TRAF6 immunoprecipitations, 10% SDS was added to cleared lysates for a final concentration of 1% SDS and boiled for 5 min. Boiled lysates were diluted 10-fold in PBS, and anti-TRAF6–coupled (Santa Cruz Biotechnology, Inc.) protein A beads (Thermo Fisher Scientific) were added. Samples were washed three times with 1× PBS and boiled in Laemmli buffer for immunoblot analysis with either antiubiquitin (P4D1; Santa Cruz Biotechnology, Inc.) or anti-TRAF6 (EMD) antibodies.

This paper is dedicated to the memory of Ken Rainin.

This work was supported by National Institutes of Health RO1 grants AI53224 and DK071939 (to A. Ma), the Rainin Foundation, fellowships from the Crohn's and Colitis

Foundation of America (to O. Hitotsumatsu) and the Association pour la Recherche sur le Cancer, the Irvington Institute Fellowship of the Cancer Research Institute (to E. Mortier), and the Fundacao para a Ciência e Tecnologia (to R.M Tavares).

The authors have no conflicting financial interests.

Submitted: 1 June 2007
Accepted: 11 January 2008

REFERENCES

1. Hooper, L.V., and J.I. Gordon. 2001. Commensal host-bacterial relationships in the gut. *Science*. 292:1115–1118.
2. Rakoff-Nahoum, S., J. Paglino, F. Eslami-Varzaneh, S. Edberg, and R. Medzhitov. 2004. Recognition of commensal microflora by toll-like receptors is required for intestinal homeostasis. *Cell*. 118:229–241.
3. Rakoff-Nahoum, S., L. Hao, and R. Medzhitov. 2006. Role of toll-like receptors in spontaneous commensal-dependent colitis. *Immunity*. 25:319–329.
4. Ting, J.P., D.L. Kastner, and H.M. Hoffman. 2006. CATERPILLERs, pyrin and hereditary immunological disorders. *Nat. Rev. Immunol*. 6:183–195.
5. Takeda, K., and S. Akira. 2004. Microbial recognition by Toll-like receptors. *J. Dermatol. Sci*. 34:73–82.
6. Takeda, K., and S. Akira. 2004. TLR signaling pathways. *Semin. Immunol*. 16:3–9.
7. Barton, G.M., and R. Medzhitov. 2003. Toll-like receptor signaling pathways. *Science*. 300:1524–1525.
8. Kawai, T., O. Adachi, T. Ogawa, K. Takeda, and S. Akira. 1999. Unresponsiveness of MyD88-deficient mice to endotoxin. *Immunity*. 11:115–122.
9. Adachi, O., T. Kawai, K. Takeda, M. Matsumoto, H. Tsutsui, M. Sakagami, K. Nakanishi, and S. Akira. 1998. Targeted disruption of the MyD88 gene results in loss of IL-1- and IL-18-mediated function. *Immunity*. 9:143–150.
10. Yamamoto, M., S. Sato, H. Hemmi, K. Hoshino, T. Kaisho, H. Sanjo, O. Takeuchi, M. Sugiyama, M. Okabe, K. Takeda, and S. Akira. 2003. Role of adaptor TRIF in the MyD88-independent toll-like receptor signaling pathway. *Science*. 301:640–643.
11. Hoebe, K., X. Du, P. Georgel, E. Janssen, K. Tabeta, S.O. Kim, J. Goode, P. Lin, N. Mann, S. Mudd, et al. 2003. Identification of Lps2 as a key transducer of MyD88-independent TIR signalling. *Nature*. 424:743–748.
12. Doyle, S., S. Vaidya, R. O'Connell, H. Dadgostar, P. Dempsey, T. Wu, G. Rao, R. Sun, M. Haberland, R. Modlin, and G. Cheng. 2002. IRF3 mediates a TLR3/TLR4-specific antiviral gene program. *Immunity*. 17:251–263.
13. Liew, F.Y., D. Xu, E.K. Brint, and L.A. O'Neill. 2005. Negative regulation of toll-like receptor-mediated immune responses. *Nat. Rev. Immunol*. 5:446–458.
14. Kobayashi, K., L.D. Hernandez, J.E. Galan, C.A. Janeway Jr., R. Medzhitov, and R.A. Flavell. 2002. IRAK-M is a negative regulator of Toll-like receptor signaling. *Cell*. 110:191–202.
15. Nakagawa, R., T. Naka, H. Tsutsui, M. Fujimoto, A. Kimura, T. Abe, E. Seki, S. Sato, O. Takeuchi, K. Takeda, et al. 2002. SOCS-1 participates in negative regulation of LPS responses. *Immunity*. 17:677–687.
16. Brint, E.K., D. Xu, H. Liu, A. Dunne, A.N. McKenzie, L.A. O'Neill, and F.Y. Liew. 2004. ST2 is an inhibitor of interleukin 1 receptor and Toll-like receptor 4 signaling and maintains endotoxin tolerance. *Nat. Immunol*. 5:373–379.
17. Wald, D., J. Qin, Z. Zhao, Y. Qian, M. Naramura, L. Tian, J. Towne, J.E. Sims, G.R. Stark, and X. Li. 2003. SIGIRR, a negative regulator of Toll-like receptor-interleukin 1 receptor signaling. *Nat. Immunol*. 4:920–927.
18. Metcalf, D., L. Di Rago, S. Mifsud, L. Hartley, and W.S. Alexander. 2000. The development of fatal myocarditis and polymyositis in mice heterozygous for IFN-gamma and lacking the SOCS-1 gene. *Proc. Natl. Acad. Sci. USA*. 97:9174–9179.
19. Marine, J.C., D.J. Topham, C. McKay, D. Wang, E. Parganas, D. Stravopodis, A. Yoshimura, and J.N. Ihle. 1999. SOCS1 deficiency causes a lymphocyte-dependent perinatal lethality. *Cell*. 98:609–616.
20. Opipari, A.W., Jr., M.S. Boguski, and V.M. Dixit. 1990. The A20 cDNA induced by tumor necrosis factor alpha encodes a novel type of zinc finger protein. *J. Biol. Chem*. 265:14705–14708.
21. Lee, E.G., D.L. Boone, S. Chai, S.L. Libby, M. Chien, J.P. Lodolce, and A. Ma. 2000. Failure to regulate TNF-induced NF-kappaB and cell death responses in A20-deficient mice. *Science*. 289:2350–2354.
22. Boone, D.L., E.E. Turer, E.G. Lee, R.C. Ahmad, M.T. Wheeler, C. Tsui, P. Hurley, M. Chien, S. Chai, O. Hitotsumatsu, et al. 2004. The ubiquitin-modifying enzyme A20 is required for termination of Toll-like receptor responses. *Nat. Immunol*. 5:1052–1060.
23. Wertz, I.E., K.M. O'Rourke, H. Zhou, M. Eby, L. Aravind, S. Seshagiri, P. Wu, C. Wiesmann, R. Baker, D.L. Boone, et al. 2004. De-ubiquitination and ubiquitin ligase domains of A20 downregulate NF-kappaB signalling. *Nature*. 430:694–699.
24. Barton, G.M., and R. Medzhitov. 2002. Control of adaptive immune responses by Toll-like receptors. *Curr. Opin. Immunol*. 14:380–383.
25. Kaisho, T., and S. Akira. 2001. Dendritic-cell function in Toll-like receptor- and MyD88-knockout mice. *Trends Immunol*. 22:78–83.
26. Fitzgerald, K.A., D.C. Rowe, B.J. Barnes, D.R. Caffrey, A. Visintin, E. Latz, B. Monks, P.M. Pitha, and D.T. Golenbock. 2003. LPS-TLR4 signaling to IRF-3/7 and NF-κB involves the Toll adapters TRAM and TRIF. *J. Exp. Med*. 198:1043–1055.
27. Fitzgerald, K.A., S.M. McWhirter, K.L. Faia, D.C. Rowe, E. Latz, D.T. Golenbock, A.J. Coyle, S.M. Liao, and T. Maniatis. 2003. IKKepsilon and TBK1 are essential components of the IRF3 signaling pathway. *Nat. Immunol*. 4:491–496.
28. Naito, A., S. Azuma, S. Tanaka, T. Miyazaki, S. Takaki, K. Takatsu, K. Nakao, K. Nakamura, M. Katsuki, T. Yamamoto, and J. Inoue. 1999. Severe osteopetrosis, defective interleukin-1 signalling and lymph node organogenesis in TRAF6-deficient mice. *Genes Cells*. 4:353–362.
29. Han, K.J., X. Su, L.G. Xu, L.H. Bin, J. Zhang, and H.B. Shu. 2004. Mechanisms of the TRIF-induced interferon-stimulated response element and NF-kappaB activation and apoptosis pathways. *J. Biol. Chem*. 279:15652–15661.
30. Deng, L., C. Wang, E. Spencer, L. Yang, A. Braun, J. You, C. Slaughter, C. Pickart, and Z.J. Chen. 2000. Activation of the IkappaB kinase complex by TRAF6 requires a dimeric ubiquitin-conjugating enzyme complex and a unique polyubiquitin chain. *Cell*. 103:351–361.
31. Rakoff-Nahoum, S., and R. Medzhitov. 2006. Role of the innate immune system and host-commensal mutualism. *Curr. Top. Microbiol. Immunol*. 308:1–18.
32. Kuhn, R., J. Lohler, D. Rennick, K. Rajewsky, and W. Muller. 1993. Interleukin-10-deficient mice develop chronic enterocolitis. *Cell*. 75:263–274.
33. Sartor, R.B. 2005. Role of commensal enteric bacteria in the pathogenesis of immune-mediated intestinal inflammation: lessons from animal models and implications for translational research. *J. Pediatr. Gastroenterol. Nutr*. 40:S30–S31.
34. Hirsch, E., V.M. Irikura, S.M. Paul, and D. Hirsh. 1996. Functions of interleukin 1 receptor antagonist in gene knockout and overproducing mice. *Proc. Natl. Acad. Sci. USA*. 93:11008–11013.
35. Rescigno, M., M. Urbano, B. Valzasina, M. Francolini, G. Rotta, R. Bonasio, F. Granucci, J.P. Kraehenbuhl, and P. Ricciardi-Castagnoli. 2001. Dendritic cells express tight junction proteins and penetrate gut epithelial monolayers to sample bacteria. *Nat. Immunol*. 2:361–367.
36. Niess, J.H., S. Brand, X. Gu, L. Landsman, S. Jung, B.A. McCormick, J.M. Vyas, M. Boes, H.L. Ploegh, J.G. Fox, et al. 2005. CX3CR1-mediated dendritic cell access to the intestinal lumen and bacterial clearance. *Science*. 307:254–258.
37. Chieppa, M., M. Rescigno, A.Y. Huang, and R.N. Germain. 2006. Dynamic imaging of dendritic cell extension into the small bowel lumen in response to epithelial cell TLR engagement. *J. Exp. Med*. 203:2841–2852.
38. Sato, S., M. Sugiyama, M. Yamamoto, Y. Watanabe, T. Kawai, K. Takeda, and S. Akira. 2003. Toll/IL-1 receptor domain-containing adaptor inducing IFN-beta (TRIF) associates with TNF receptor-associated factor 6 and TANK-binding kinase 1, and activates two distinct transcription factors, NF-kappa B and IFN-regulatory factor-3, in the Toll-like receptor signaling. *J. Immunol*. 171:4304–4310.

39. Meylan, E., K. Burns, K. Hofmann, V. Blancheteau, F. Martinon, M. Kelliher, and J. Tschopp. 2004. RIP1 is an essential mediator of Toll-like receptor 3-induced NF-kappa B activation. *Nat. Immunol.* 5:503–507.
40. Cusson-Hermance, N., S. Khurana, T.H. Lee, K.A. Fitzgerald, and M.A. Kelliher. 2005. Rip1 mediates the Trif-dependent toll-like receptor 3- and 4-induced NF-{kappa}B activation but does not contribute to interferon regulatory factor 3 activation. *J. Biol. Chem.* 280:36560–36566.
41. Song, H.Y., M. Rothe, and D.V. Goeddel. 1996. The tumor necrosis factor-inducible zinc finger protein A20 interacts with TRAF1/TRAF2 and inhibits NF-kappaB activation. *Proc. Natl. Acad. Sci. USA.* 93:6721–6725.
42. Wang, Y.Y., L. Li, K.J. Han, Z. Zhai, and H.B. Shu. 2004. A20 is a potent inhibitor of TLR3- and Sendai virus-induced activation of NF-kappaB and ISRE and IFN-beta promoter. *FEBS Lett.* 576:86–90.
43. Saitoh, T., M. Yamamoto, M. Miyagishi, K. Taira, M. Nakanishi, T. Fujita, S. Akira, N. Yamamoto, and S. Yamaoka. 2005. A20 is a negative regulator of IFN regulatory factor 3 signaling. *J. Immunol.* 174:1507–1512.
44. Oganesyan, G., S.K. Saha, B. Guo, J.Q. He, A. Shahangian, B. Zarnegar, A. Perry, and G. Cheng. 2006. Critical role of TRAF3 in the Toll-like receptor-dependent and -independent antiviral response. *Nature.* 439:208–211.
45. Hacker, H., V. Redecke, B. Blagoev, I. Kratchmarova, L.C. Hsu, G.G. Wang, M.P. Kamps, E. Raz, H. Wagner, G. Hacker, et al. 2006. Specificity in Toll-like receptor signalling through distinct effector functions of TRAF3 and TRAF6. *Nature.* 439:204–207.
46. Yuan, J.S., and C. Neal Stewart Jr. 2005. Real-time PCR statistics. *PCR Encyclopedia.* 1:101127–101149.